

Stability evaluation for the excavation face of shield tunnel across the Yangtze River by multi-factor analysis

Yiguo Xue, Xin Li, Daohong Qiu*, Xinmin Ma, Fanmeng Kong, Chuanqi Qu and Ying Zhao

Geotechnical and Structural Research Center of Shandong University, Jinan, Shandong, China

(Received July 9, 2019, Revised October 16, 2019, Accepted October 22, 2019)

Abstract. Evaluating the stability of the excavation face of the cross-river shield tunnel with good accuracy is considered as a nonlinear and multivariable complex issue. Understanding the stability evaluation method of the shield tunnel excavation face is vital to operate and control the shield machine during shield tunneling. Considering the instability mechanism of the excavation face of the cross-river shield and the characteristics of this engineering, seven evaluation indexes of the stability of the excavation face were selected, i.e., the over-span ratio, buried depth of the tunnel, groundwater condition, soil permeability, internal friction angle, soil cohesion and advancing speed. The weight of each evaluation index was obtained by using the analytic hierarchy process and the entropy weight method. The evaluation model of the cross-river shield construction excavation face stability is established based on the idea point method. The feasibility of the evaluation model was verified by the engineering application in a cross-river shield tunnel project in China. Results obtained via the evaluation model are in good agreement with the actual construction situation. The proposed evaluation method is demonstrated as a promising and innovative method for the stability evaluation and safety construction of the cross-river shield tunnel engineering.

Keywords: cross-river tunnel; shield construction; stability of the excavation face; AHP-entropy weight method; ideal point evaluation model

1. Introduction

Underwater tunnels are widely utilized in underwater engineering owing to their ability to withstand war damage and natural disasters. With the development of the tunnel construction technology, cross-river tunnels have gradually become the focus of underground engineering construction (Jiang and Wu 2015). As the most advanced tunnel construction technology, shield tunneling has been widely used in urban underground engineering construction due to its advantages, such as high excavation rate, strong safety and small environmental disturbances. During shield tunneling, support pressure is applied to the excavation face to balance the water and earth pressure on the excavation face. Large-diameter shield tunnels are faced with so complex hydrogeology that tunneling schemes are difficult to carry out. Due to the instability of the excavation face, the water inrush, sand gushing and surface subsidence of the shield tunnels occur frequently (Sousa and Einstein 2012, Hong *et al.* 2009). The endless emergence of the shield tunnel accidents delays the progress of projects and causes inestimable losses. Therefore, it is essential to ensure the safety of shield construction. For cross-river tunnels, the control of the excavation face stability is the most important work of the project. At present, three methods i.e., the model experiment, the numerical simulation, and non-linear theory are commonly used to investigate the stability of the

Table 1 Stability coefficient method classification (Attewell 1971)

Stability grade	Stability coefficient N	Deformation description
I	<1	Negligible
II	1~2	Elastic deformation
III	2~4	Elastoplastic deformation
IV	4~6	Plastic deformation
V	>6	Instability failure

excavation face.

Broms and Benermark (1967) first proposed the classical concept of the stability coefficient of the excavation face and obtained a formula (see Eq.(1)) for calculating the stability coefficient of the excavation face.

$$N = \frac{\delta_s + \gamma(C + D/2) - \delta_t}{C_U} \quad (1)$$

where N is the stability coefficient of the excavation face, δ_t represents the support pressure and δ_s represents the ground overload. C is the distance from the surface to the axis of the shield cutter. γ is the weight of the soil in front of the excavation and C_U represents the undrained shear strength index of the soil in the tunnel center. Attewell conducted an in-depth study and established the evaluation standards of the stability of the excavation face (Table 1), the higher the stability coefficient, the higher the stability degree of the excavation face.

The limit analysis method is a new method in investigating the excavation face stability and is widely

*Corresponding author, Ph.D.
E-mail: qdh2011@126.com

used in geotechnical engineering (Viratjandr and Michalowski 2006, Kim *et al.* 2002, Li and Yang 2019). The influence of seepage is crucial in the study of the excavation face stability of the cross-river tunnel, while the limit analysis method tends to ignore the influence of seepage on the stability of the excavation face (Srivastava *et al.* 2010, Shin *et al.* 2010, Coli *et al.* 2008). Perazzelli *et al.* (2014) improved the traditional limit equilibrium formula and studied the stability of the tunnel excavation face under seepage conditions. This study provides an important reference for the study on the influence of seepage on the excavation face stability. Engineering application is a crucial way to verify theoretical research results and can optimize the theoretical methods as well. Taking the Shanghai Yangtze River tunnel as an example, Li *et al.* (2009) studied the local and overall failure mechanism of the working face of a large slurry shield tunnel by combining limit analysis and the upper-limit method of a three-dimensional numerical simulation, which provides a comprehensive reference for shield construction. Due to the subway project of Xuzhou City in China, Song *et al.* (2018) proposed the targeted design of shield selection and the selection of excavation parameters. Numerical simulation methods have become widely used according to the development of software technology. Discrete element numerical simulation and Flac3d are commonly used numerical simulation methods (Shu *et al.* 2011, Hasanpour 2014, Duan *et al.* 2018, Kim *et al.* 2018, Li *et al.* 2018). Maynar and Rodríguez (2005) used the DEM to establish a discrete numerical model for the excavation analysis of earth pressure balance tunnels. Since the cost of the field experiments is high, and the numerical simulation method cannot accurately determine the process of excavation face instability. Therefore, an efficient and low-cost method is now urgently needed. Due to the advantages of saving time, being easy to perform, the model test has become a practical way to verify and deepen the theoretical calculations. The three-dimensional model test is the focus of the model test (Chen *et al.* 2013, Ma *et al.* 2017, Kong and Shang 2018). However, due to the requirements of sampling in the complex conditional field, the results of the model test will be inevitably disturbed by sampling, preservation and preparation. The test process thus easily causes the errors of the calculation. Therefore, it is of considerable significance for shield construction to establish a grading evaluation system for evaluating the stability of the excavation face considering actual construction factors.

This paper innovatively applied the ideal point method to the stability evaluation of the excavation face of the cross-river shield tunnel. On the basis of studying the failure mechanism of the excavation face instability, the author selected seven evaluation indexes for the excavation face stability (Anagnostou and Kovári 1996, Zhang *et al.* 2017). The combination weight of the evaluation indexes was determined by the analytic hierarchy process and entropy weight methods. The final evaluation model was established by the ideal point method. Finally, the evaluation result of the ideal point was compared with the calculation result of the classical stability coefficient method and the actual grade of the construction site to verify the feasibility of the model.

2. Weight calculation method

In a decision-making system, it is necessary to emphasize the universality and being easy to obtain in the process of selecting the influencing factors. Moreover, weight calculation is the most crucial method to obtain the influence degree of the decision-factor on the target attributes. In this paper, the analytic hierarchy process and entropy weight method are used to determine the combination weight of the evaluation indexes.

2.1 Analytic hierarchy process

There are usually multiple decision attributes in the process of evaluating a specific target attribute, which may increase the difficulty of the decision-making process. Hence, it is necessary to rank the importance of these indicators according to their influence on the decision-making results. The analytic hierarchy process method refers to the paired comparison of evaluation indexes, and a scale from 1 to 9 is taken as the standard of the indicator importance evaluation by decision-makers (Kim *et al.* 2014). In Eq.(2), the judgment matrix $G_{n \times n}$ is constructed based on the AHP method to rank the overall importance of the indicators (Hyun *et al.* 2015, Aalianvari *et al.* 2012, Katibeh and Aalianvari 2009, Hamidi 2010).

$$G_{n \times n} = \begin{bmatrix} I_{1 \rightarrow 1} & I_{1 \rightarrow 2} & \dots & I_{1 \rightarrow n} \\ I_{2 \rightarrow 1} & I_{2 \rightarrow 2} & \dots & I_{2 \rightarrow n} \\ \vdots & \vdots & \ddots & \vdots \\ I_{n \rightarrow 1} & I_{n \rightarrow 2} & \dots & I_{n \rightarrow n} \end{bmatrix} \quad (2)$$

where $I_{i \rightarrow j}$ is the importance of the i_{th} evaluation index I_i relative to the j_{th} evaluation index I_j . The degree of influence of the evaluation indexes on the decision-making results is quantitatively expressed with a scale from 1 to 9 in Table 2.

In Table 2, $I_{i \rightarrow j}$ indicates the importance of the i_{th} index relative to the j_{th} index. Similarly, the importance degree of the j_{th} index relative to the i_{th} index is $1/I_{i \rightarrow j}$. In this paper, the maximum eigenvalue method is used to obtain the maximum eigenvalue and the corresponding eigenvector of the judgment matrix.

$$G \cdot u = \lambda_{\max} \cdot u \quad (3)$$

The maximum eigenvalue λ_{\max} and its eigenvector u are obtained according to Eq. (3). To avoid contradictions in the importance ranking process due to multi-factors in the

Table 2 Value of $I_{i \rightarrow j}$

Value of $I_{i \rightarrow j}$	Meaning of the value
1	I_i and I_j are equally important.
3	I_i is slightly more important than I_j .
5	I_i is obviously more important than I_j .
7	I_i is much more important than I_j .
9	I_i is extremely more important than I_j .
2,4,6,8	Intermediate value of the above adjacent judgment.

Table 3 Value of RI

Order (n)	1	2	3	4	5	6	7	8	9
RI	0.00	0.00	0.58	0.90	1.12	1.24	1.32	1.41	1.45

decision-making process, the consistency test coefficient CR was introduced and defined (Eq. (4)).

$$CR = CI / RI \tag{4}$$

where CI is the consistency index, which can be used to measure the degree of inconsistency of $G_{n \times n}$ and can be obtained by Eq. (5). Furthermore, the random consistency index RI was defined as shown in Table 3, where n is the number of the indexes.

$$CI = (\lambda_{max} - n) / (n - 1) \tag{5}$$

Finally, the decision process is evaluated according to the value of CR. When $CR < 0.1$, it can be considered that the judgment matrix $G_{n \times n}$ has acceptable consistency, and the weight vector $w_i = (w_1, w_2, w_3, \dots, w_n)$ can be obtained by normalizing the eigenvector u corresponding to the maximum eigenvalue λ_{max} (Eq. (6)).

$$w_i = u_i / \sum_{i=1}^n u_i \tag{6}$$

where $0 \leq w_i \leq 1$, and $\sum_{i=1}^n w_i = 1$. In contrast, when $CR \geq 0.1$, it is considered that the degree of deviation from the consistency of the judgment matrix is so large that the element value in G needs to be modified.

2.2 Entropy weight method

The entropy weight method determines the weights of the decision-factors according to the amount of information contained in each indicator in the decision-making system. In the process of calculating the weights of the different decision-factors, the entropy weight method mainly analyzes the variability degree of each decision-factors in the decision-making system. The greater the variability of the decision-factors, the more the information contained in the indicators. Finally, the information reflected by the sample data is defined as the entropy, and the objective weight of the evaluation indicator is determined based on the entropy value of the sample data. The entropy weight method is used to determine the weight of the indicator as the following steps (Constantin *et al.* 2011, Felicísimo *et al.* 2013, Delgado and Romero 2016).

2.2.1 Normalization of the data samples

Assuming that the number of the evaluation index is m and the count of the objects to be evaluated is n, the data sample matrix $M(x_{ij})_{m \times n}$ is obtained. To avoid the influence of the dimension of the evaluation index on the calculation results, the value of each index in the matrix $M(x_{ij})_{m \times n}$ needs to be normalized. The positive index means that the larger the index is, the more stable the excavation face will be. For a positive index x^+_{ij} , the data are normalized according to

Eq. (7). For the negative index x^-_{ij} , the larger the index is, the more unstable the excavation face will be. The data are normalized according to Eq. (8) for the negative index.

$$r_{ij} = \frac{x^+_{ij} - \min(x^+_j)}{\max(x^+_j) - \min(x^+_j)} \tag{7}$$

$$r_{ij} = \frac{\max(x^-_j) - x^-_{ij}}{\max(x^-_j) - \min(x^-_j)} \tag{8}$$

where x_{ij} is the i_{th} value of the j_{th} index, the r_{ij} represents the normalized value.

2.2.2 Define entropy

Since there are m indexes and n objects to be evaluated in the decision-making system, and the entropy H_i of the i_{th} index can be defined as Eq. (9).

$$H_i = -K \sum_{j=1}^n f_{ij} \ln f_{ij} \tag{9}$$

where $K = 1 / \ln n$, Eq. (10) was used to determine f_{ij} .

$$f_{ij} = r_{ij} / \sum_{j=1}^n r_{ij} \tag{10}$$

Since r_{ij} is the j_{th} valid value corresponding to the i_{th} index and m is the number of the index, it is unnecessary to consider the case that $f_{ij} = 0$.

2.2.3 Define entropy weight

Finally, on the basis of obtaining the entropy value of the evaluation index, the entropy weight vector $e_i (e_1, e_2, e_3, \dots, e_m)$ of the index is defined by Eq. (11).

$$e_i = \frac{1 - H_i}{m - \sum_{i=1}^m H_i} \tag{11}$$

where $0 \leq e_i \leq 1, \sum_{i=1}^m e_i = 1$.

2.3 Combination weights

In order to prevent the subjectivity of the weight results caused by the analytic hierarchy process and the contingency of the weight calculation results caused by the entropy weight method, the distribution coefficients are introduced to reasonably allocated the two types of weights to obtain the combination weight. The distance function $f(x)$ is introduced to calculate the distribution coefficients of the weights according to Eqs. (12)-(14).

$$\begin{cases} f(w_i, e_i) = \left[\frac{1}{2} \sum_{i=1}^n (w_i - e_i)^2 \right]^{\frac{1}{2}} \\ (\alpha - \beta)^2 = \frac{1}{2} \sum_{i=1}^n (w_i - e_i)^2 \end{cases} \tag{12}$$

Assume that the combination weight is W_i . According to Eq.(13), the final combined weight value is obtained.

$$W_i = \alpha w_i + \beta e_i \tag{13}$$

where α and β are the distribution coefficients of the weights. Moreover, Eq. (14) is proposed as a constraint condition.

$$\alpha + \beta = 1 \tag{14}$$

Finally the combination weight W_i is calculated by substituting the distribution coefficient α and β into Eq. (13).

3. Evaluation model of the ideal point method

The ideal point method, also known as the Topsis method, is a multi-factor decision-making method. In this method, the evaluation result is obtained by calculating the closeness between the decision object and the decision attribute. The most suitable solution with a positive ideal solution has the shortest distance. The ideal point method has been applied in many fields, i.e., the grade division of the surrounding rock of the tunnel, the site selection evaluation of underground engineering and the quantitative assessment of the tunnel damage (Wang *et al.* 2016, Li *et al.* 2017).

In this paper, the ideal point method is used to construct the evaluation model for evaluating the excavation face stability. After established the stability grading evaluation system, the positive ideal point and the anti-ideal point of the target attribute are constructed by comprehensively considering the characteristics of the indexes. The closeness degree of the evaluation index to the ideal points of different grades is regarded as the criterion for decision-making. The calculation process of the ideal point method is as follows.

3.1 Establish the stability evaluation system

Assuming that the number of the evaluation index is m and the count of the objects to be evaluated is n . The excavation face stability decision matrix $Q_{m \times n}$ will be obtained with m rows and n columns as the following matrix (see Eq. (15)).

$$Q_{m \times n} = \begin{pmatrix} q_{1,1} & q_{1,2} & \dots & q_{1,n} \\ q_{2,1} & q_{2,2} & \dots & q_{2,n} \\ \dots & \dots & \dots & \dots \\ q_{m,1} & q_{m,2} & \dots & q_{m,n} \end{pmatrix} \tag{15}$$

Suppose that the grade set $U = \{u_1, u_2, \dots, u_k\}$ can be described as the target attribute set. In the decision-making process of the excavation face stability, U represents the excavation face stability. Thus the stability grade of the excavation can be divided into k grades. Correspondingly, the value ranges of indexes were all divided into k intervals which constituted the grading evaluation system for evaluating the stability of the excavation face.

3.2 Determine the positive and anti-ideal ideal points

The evaluation index for evaluating the stability of the excavation face can be divided into the positive index and negative index. The positive index indicates that as the index value increases, the stability of the excavation surface is increased and the risk is decreased. The negative index means that as the index value decreases, the stability of the excavation face is decreased and the risk is increased. When the evaluation index q_i^+ of the excavation face stability is the positive index, the positive ideal point (A^+) and the anti-ideal point (A^-) are determined by Eq. (16).

$$\begin{cases} A_i^+ = \{q_{i1}^+, q_{i2}^+, \dots, q_{in}^+\} = \{\max(q_{ij}^+)(j = 1, 2, \dots, n)\} \\ A_i^- = \{q_{i1}^+, q_{i2}^+, \dots, q_{in}^+\} = \{\min(q_{ij}^+)(j = 1, 2, \dots, n)\} \end{cases} \tag{16}$$

When the evaluation index q_i^- is the negative index, the positive ideal point (A^+) and the anti-ideal point (A^-) of the negative index q_i^- are obtained from Eq.(17).

$$\begin{cases} A_i^+ = \{q_{i1}^-, q_{i2}^-, \dots, q_{in}^-\} = \{\min(q_{ij}^-)(j = 1, 2, \dots, n)\} \\ A_i^- = \{q_{i1}^-, q_{i2}^-, \dots, q_{in}^-\} = \{\max(q_{ij}^-)(j = 1, 2, \dots, n)\} \end{cases} \tag{17}$$

3.3 The ideal point evaluation function

The ideal point evaluation function $D(x)$ is introduced to calculate the distance between the value of the evaluation index and the ideal point. The distance from the index q_i to the positive ideal point A^+ can be expressed as Eq. (18).

$$D_i^+ = \left\{ \sum_{i=1}^m W_i \left[\frac{q_i - A_i^+}{|q_{imax} - q_{imin}|} \right]^2 \right\}^{\frac{1}{2}} \tag{18}$$

The distance from the index q_i to the anti-ideal point A^- can be expressed as Eq. (19).

$$D_i^- = \left\{ \sum_{i=1}^m W_i \left[\frac{q_i - A_i^-}{|q_{imax} - q_{imin}|} \right]^2 \right\}^{\frac{1}{2}} \tag{19}$$

where q_{imax} and q_{imin} are the upper and lower limits of the range of the different stability grades of each evaluation index respectively.

3.4 Ideal point grade closeness degree

Since the stability grade of the excavation can be divided into k grades. The ideal point closeness degree $T_i \{T_1, T_2, \dots, T_k\}(i=1, 2, 3, \dots, k)$ is obtained according to the Eq. (20).

$$T_i = \frac{D_i^+}{D_i^+ + D_i^-} \tag{20}$$

According to Eq. (20), the ideal point closeness degree T is in the interval station $[0,1]$. If T is increased, then the distance to the positive ideal point is decreased and the distance to the negative ideal point is increased. Finally, the

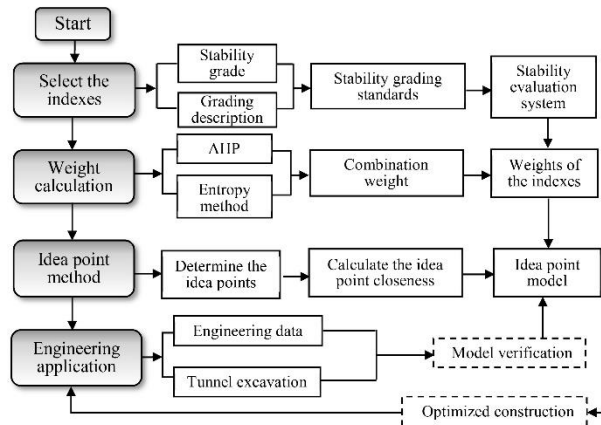


Fig. 1 Methodological flowchart of the comprehensive evaluation model

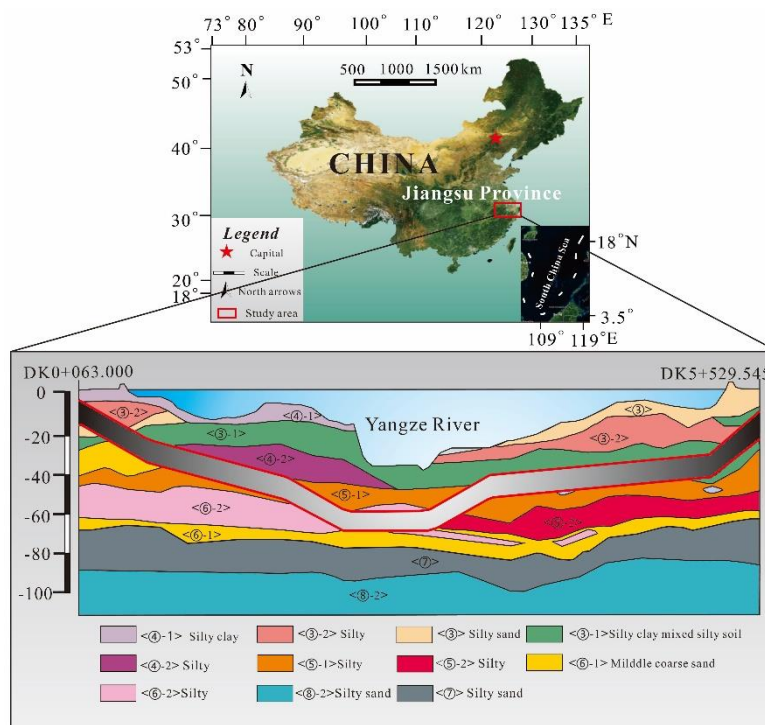


Fig. 2 Geographical location of the tunnel. Adapted from Li *et al.* (2019)

stability grade corresponding to the maximum closeness degree of the calculated results is used as the evaluation result. If $T_k = \max T_i \{T_1, T_2, \dots, T_k | i = 1, 2, \dots, k\}$, grade k is the evaluation grade. In this paper, the content of the research is to comprehensively evaluate the stability of the excavation face of the shield tunnel. In summary, the methodological flowchart of the comprehensive evaluation model can be described in Fig. 1.

4. Case study

4.1 Project summary

The project is located in Jiangsu Province, China. The construction route of the project runs north from the original well of the south bank of the Yangtze River, and then enters the Yangtze River channel through the south

bank of the Yangtze River. Finally, the shield arrived at the receiving well of the north bank. The lowest elevation of the tunnel structure is -74.83 m, and the maximum water pressure is 0.80 MPa. Fig. 2 shows that the total length of the shield tunnel is 5,466.545 m.

Fig. 2 gives a description of the longitudinal section of the tunnel. The tunnel is located in the alluvial geological subarea (area II 1) south of the Yangtze River. The depth of the tunnel in this section is all quaternary soil layers. The division of the strata is based on the geological age, genesis, lithology and other geological features of the soil.

4.2 Excavation face stability evaluation model

In a multi-indicator decision-making process, the process of selecting the indexes needs to emphasize the universality and being easy to obtain. Considering the reasons for the instability of the excavation face during

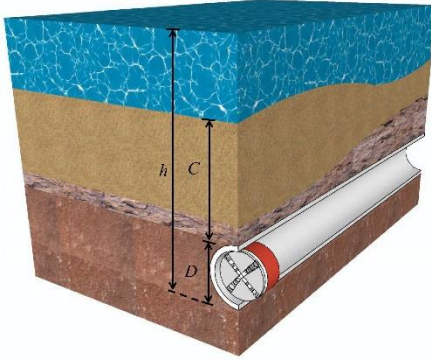


Fig. 3 Description of the over-span ratio. Adapted from Li *et al.* (2019)

Table 4 Grading standards of the soil permeability

Grade	Permeability coefficient λ (cm/s)	Quantitative standard
I	$>10^{-1}$	0.8~1.0
II	$10^{-1} \sim 10^{-3}$	0.6~0.8
III	$10^{-3} \sim 10^{-5}$	0.4~0.6
IV	$10^{-5} \sim 10^{-7}$	0.2~0.4
V	$<10^{-7}$	0~0.2

Table 5 Grading standards of the advancing speed

Grade	Description of the speed	Advancing speed(mm/min)
I	Very fast	80~100
II	Fast	60 ~ 80
III	Slow	40 ~ 60
IV	Very slow	20 ~ 40
V	Basically stagnant	0~20

shield tunneling and the principle of shield construction control, the author selected the following evaluation indicators for evaluating the stability of the excavation face. The influencing factors of the excavation face stability are described as follows.

(1) Buried depth of the tunnel h

To date, a large number of cross-river tunnel projects have emerged. The complex distributions of the water and soil pressures have a great influence on the stability of the excavation face. The support pressure can not balance the water and earth pressure on the excavation face, this will cause the instability of the excavation face. Thus the larger the buried depth h of the tunnel, the larger the water and earth pressure on the excavation, and the greater the risk of the excavation face instability (Fig. 3).

(2) Over-span ratio e

During shield tunneling, e refers to the ratio between the overburden thickness C of the tunnel and the tunnel diameter D (Fig. 3), namely C/D . The over-span ratio determines the influence degree of the water and soil pressure on the tunnel stability to some extent (Hatzor and Corte 2010). When the over-span ratio increases, the disturbance degree of the soil and water around the tunnel will also increase, which will increase the instability risk of the excavation face (Su *et al.* 2019).

(3) Internal friction angle φ

The internal friction angle φ is an important shear strength index of the rock soil, and it is also an important parameter to evaluate the stability of the excavation face during construction. The shield tunneling machine maintains the stability of the excavation face by providing support pressure acting on the mud film formed in front of the excavation face. Generally speaking, the larger the internal friction angle, the more stable the mud film on the excavation surface (Chambon and Corte 1994).

(4) Cohesion of soil c

The cohesion of soil c is an important evaluation index of the excavation face stability. The soil with a high cohesion can easily form a stable mud film on the excavation face and improve the strength of the excavation face. In this paper, c is taken as an evaluation index for the stability evaluation of the excavation face (Khezri *et al.* 2010).

(5) Groundwater condition w

For an underwater tunnel, the influence of the groundwater on the stability of the excavation face is due to the influence of the water content on the excavation face. The high water content in front of the excavation face during construction will break through the excavation face and cause the instability of the excavation face. Many engineering examples have shown that the instability risk of excavation faces is higher under geological conditions with higher groundwater content. Therefore, groundwater is used as a factor to evaluate the stability of the excavation face of shield construction, and the natural water content of the soil is used as an evaluation index of the groundwater content (Wu and Zhao 2015, Ma and Zoback 2018).

(6) Soil permeability p

The mechanism of the stability of the excavation face of the shield tunnel indicates that the soil mass of the excavation face has a small permeability, the excavation face can easily form a stable mud film, and the excavation face has high stability. In contrast, the permeability of soil on the excavation face is high, and the stability of the excavation face will be poor (Lee *et al.* 2004). Due to the large difference in soil permeability coefficient between the middle and lower reaches of the Yangtze River, the permeability p is obtained according to Eq.(21). Table 4 shows the grading standards of the soil permeability.

$$p = a_K + (\lambda - b_K) / \lambda \quad (21)$$

where a_K is the upper limit of the quantitative standard of permeability grade K , b_K is the upper limit of the quantitative standard of permeability grade K . λ represents for the permeability coefficient, p is the quantitative result of the permeability of the soil.

(7) Advancing speed v

The normal advancing speed of the shield machine under the safe condition of the excavation face is generally 20-50 mm/min. At present, the fastest speed of the slurry shield advancing is more than 90 mm/min. The advancing speed of the shield machine may indicate the stability of the excavation face during shield tunneling (Culí *et al.* 2016). The advancing speed of the shield is relatively fast in low-risk sections but relatively slow or even stagnant in high-

Table 6 Grading standards of the indexes for excavation face stability evaluation

Index	Stability grades for the excavation face				
	Extremely high (I)	High (II)	Medium (III)	Slight (IV)	Weak (V)
e	0~1.5	1.5~3.0	3.0~4.5	4.5~6	6~10
h (m)	0~30	30~60	60~90	90~150	150~250
c (kPa)	40~55	30~40	20~30	10~20	0~10
φ (°)	40~50	30~40	20~30	10~20	0~10
v (mm/min)	80~100	60~80	40~60	20~40	0~20
w (%)	0~10	10~20	20~30	30~40	40~60
p	0~0.2	0.2~0.4	0.4~0.6	0.6~0.8	0.8~1.0

Table 7 The description of the stability grade of the excavation face

Stability grade	The description
Extremely high (Grade 1)	The stability of the excavation face is extremely high. There is no obvious change in sensor parameters obtained from the shield cutter head. The construction plan remains unchanged. The cumulative deformation of the segments at the excavation face is less than 15mm per day.
High (Grade 2)	The stability of the excavation face is high. The change of the sensor parameters obtained from the cutter head is not obvious. The cumulative deformation of the segments at the excavation face may reach to 15~35 mm per day.
Medium (Grade 3)	The stability of the excavation face is medium. The maximum deformation value of the segments of the tunnel is more than 55 mm per day, which beyond the normal range. The deformation monitoring of the segments and on-site recording should be strengthened to analyze whether the deformation value of the segment and the sensor parameters obtained from the cutter head are abnormal.
Slight (Grade 4)	The stability of the excavation face is slight. The deformation value of the segments of the tunnel may change abnormally. The strength of the support and the frequency of on-site monitoring should be increased appropriately. Adjust the support pressure according to the grade of the over-span ratio, and adjust the reinforcement scheme of the excavation face according to the grade of the water content.
Weak (Grade 5)	The stability of the excavation face is weak. The torque of the cutter head suddenly increases, and the water and the soil pressure suddenly increases as well. There may be cracks on the segment near the excavation. Water seepage may occur near the segments. The excavation face may be instability, and water inrush may occur near the excavation face. The construction site should stop excavation immediately.

risk areas. As shown in Table 5, the advancing speed of the shield tunneling can be divided into five grades by quantifying the advancing speed.

In conclusion, the data samples of the buried depth of

Table 8 Analytic hierarchy process decision table

Index	e	h	φ	c	v	w	p	weight
e	1	1	3	3	4	2	2	0.251
h	1	1	3	3	4	2	2	0.251
φ	1/3	1/3	1	1	2	1/2	1/2	0.081
c	1/3	1/3	1	1	2	1/2	1/2	0.081
v	1/4	1/4	1/2	1/2	1	1/3	1/3	0.050
w	1/2	1/2	1/3	1/3	1/4	1	1	0.143
p	1/2	1/2	1/3	1/3	1/4	1	1	0.143

Table 9 Learning samples of the evaluation indexes

Samples	Evaluation indexes						
	e	h (m)	φ (°)	c (kPa)	v (mm/min)	w (%)	p
1	0.57	6.7	15.5	15.2	16	32.8	0.41
2	1.08	12.5	19.3	38.3	34.8	30.6	0.48
3	1.48	17.2	25	29.8	33.8	33.8	0.25
4	1.91	24.2	23	37.3	30.2	38.8	0.31
5	2.22	27.8	27.9	33.5	30.3	34.2	0.52
6	2.38	30.8	26.5	34.7	27	34.6	0.48
7	2.45	31.7	26.5	33.5	28	34.6	0.38
8	3.83	48.1	33.3	10.5	34.2	22.5	0.45
9	2.57	64.5	32.5	8.8	35.1	19.6	0.45
10	2.42	57.3	31	10	34.8	33.4	0.4
11	1.84	58.2	33	24.6	44	32.8	0.36
12	2.15	46.4	33.2	20.1	35.7	33.6	0.25
13	1.88	47.2	28.8	24.8	36.1	28.9	0.25
14	2.38	47.7	26.2	12.5	30	34.8	0.28
15	2.64	48.1	25	25.7	33.4	32.8	0.31

the tunnel h , over-span ratio e , internal friction angle φ , cohesion of soil c , permeability coefficient λ and groundwater condition w are obtained from the geological exploration data. The data samples of advancing speed v can be obtained from the site construction record. This paper uses nonlinear methods and data mining to analyze the factors of excavation face stability and takes the factors as the evaluation indexes of stability evaluation. Grading standards are determined based on the characteristics of this engineering, the stability of the excavation face is divided into five grades: extremely high(I), high(II), medium (III), slight (IV) and weak(V). Correspondingly, the value ranges of evaluation indexes were divided into equal intervals to constituted the grading standards (Table 6). Since the grading standard for the excavation face of the cross-river shield tunnel has not been established in the current researches. According to the construction site research and experts' suggestions in related fields, the descriptions of the excavation face stability of different grades are listed in Table 7 (Ahmed and Iskander 2012, Dias and Kastner 2013).

4.3 Weight calculation

After establishing the grading standards of the indexes

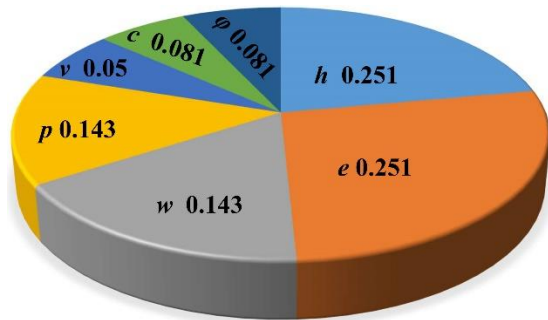


Fig. 4 Subjective weight

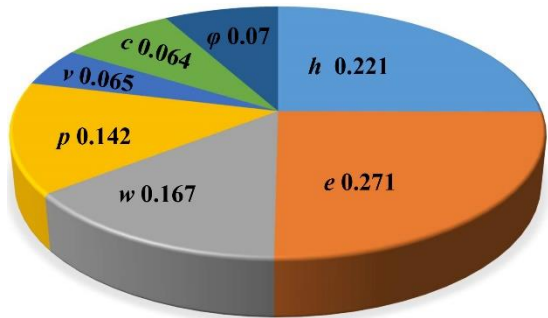


Fig. 5 Objective weight

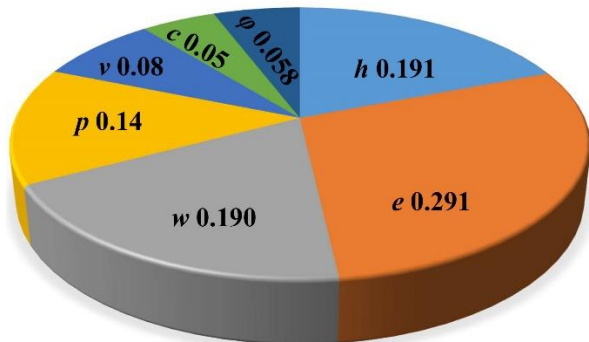


Fig. 6 Combination weight

Table 10 Samples for testing the model

Samples	Evaluation indexes						
	<i>e</i>	<i>h</i> (m)	φ (°)	<i>c</i> (kPa)	<i>v</i> (mm/min)	<i>w</i> (%)	<i>p</i>
1	2.37	40.5	26	35.5	33.8	31.2	0.29
2	1.78	39.1	31.6	21.8	35	33.6	0.46
3	2.68	68.8	28.5	11.8	29	34.5	0.58
4	1.84	44.2	33.2	5	31.8	27	0.4
5	2.34	46.5	29	24.5	37.6	31.3	0.31

for excavation face stability evaluation, the weight of the evaluation index should be calculated to obtain the degree of the influence of different indexes on the stability of the excavation face. In this paper, the AHP method is used to calculate the subjective weight of the evaluation index according to Eqs. (3)-(6). The analytic hierarchy process decision table of the evaluation indexes is shown in Table 8.

According to Eqs. (3)-(6), it can be concluded that $\lambda_{max}=7.04729$, $n=7$, $CI=0.0079$, $RI=1.32$. Since $CR=CI/RI=0.00598<0.1$, the consistency of this decision-

Table 11 Evaluation results of the excavation face stability

Samples	Closeness degree to the ideal point					Evaluation grade	Stability coefficient	Actual grade
	T_1	T_2	T_3	T_4	T_5			
1	0.6080	0.6402	0.3936	0.3119	0.3730	II	II	II
2	0.6058	0.6060	0.5072	0.3110	0.3743	I-II	III	II
3	0.5896	0.6483	0.6477	0.3117	0.3468	II~III	V	III
4	0.5994	0.5993	0.5233	0.3255	0.3757	I-II	IV	III
5	0.6105	0.6471	0.4089	0.3010	0.3723	II	IV	II

making process is considered acceptable. The subjective weight of the evaluation index (Fig. 4) is obtained according to Eq.(6).

The entropy weight method was used to calculate the objective weight of the evaluation index according to Eqs. (7)-(11). Since the entropy weight method mainly analyzes the variability degree of each evaluation index in the process of weight calculation. Fifteen learning samples were established based on the real data obtained from the cross-river shield tunnel engineering (Table 9). The learning samples in Table 9 were used to obtain objective weights according to Eqs. (7)-(11). The results can be seen in Fig. 5.

On the basis of obtaining the subjective weight and the objective weight, the weight distribution coefficient α and β is calculated according to Eq. (12). The calculation results indicated that the weight distribution coefficients are 0.502 and 0.498 respectively. Finally, the combination weight W_i (Fig. 6) is obtained by substituting the weight distribution coefficients into Eq. (13).

4.4 Engineering application

On the basis of grading standards of the indexes for excavation face stability evaluation and the comprehensive weight of the evaluation indexes, the feasibility of the stability evaluation method of the excavation face is verified by the actual engineering application. The five sets of data samples of the evaluation indexes of the cross-river shield tunnel engineering in Jiangsu Province were listed in Table 10. The data samples matrix $S_{5 \times 7}$ was obtained in Eq (22).

$$S = \begin{pmatrix} 2.37 & 40.5 & 26 & 35.5 & 33.8 & 31.2 & 0.29 \\ 1.78 & 39.1 & 31.6 & 21.8 & 35 & 33.6 & 0.46 \\ 2.68 & 68.8 & 28.5 & 11.8 & 29 & 34.5 & 0.58 \\ 1.84 & 44.2 & 33.2 & 5.0 & 31.8 & 27 & 0.4 \\ 2.34 & 46.5 & 29 & 24.5 & 37.6 & 31.3 & 0.31 \end{pmatrix} \quad (22)$$

In summary, the three indexes of the internal friction angle φ , cohesion *c* and advancing speed *v* are positive indexes, and the remaining 4 indexes are all negative indexes. Hence, the positive ideal point matrix $A^+_{5 \times 7}$ and the anti-ideal point matrix $A^-_{5 \times 7}$ of the evaluation model are as follows

$$A^+ = \begin{pmatrix} 0 & 0 & 55 & 50 & 100 & 0 & 0 \\ 1.5 & 30 & 40 & 40 & 80 & 10 & 0.2 \\ 3 & 60 & 30 & 30 & 60 & 20 & 0.4 \\ 4.5 & 90 & 20 & 20 & 40 & 30 & 0.6 \\ 6 & 120 & 10 & 10 & 20 & 40 & 0.8 \end{pmatrix} \quad (23)$$

$$A^{-} = \begin{pmatrix} 1.5 & 30 & 40 & 40 & 80 & 10 & 0.2 \\ 3 & 60 & 30 & 30 & 60 & 20 & 0.4 \\ 4.5 & 90 & 20 & 20 & 40 & 30 & 0.6 \\ 6 & 120 & 10 & 10 & 20 & 40 & 0.8 \\ 10 & 200 & 0 & 0 & 0 & 60 & 1 \end{pmatrix} \quad (24)$$

Based on the weights and the evaluation system, the stability evaluation results of the excavation face of the five sections are listed in Table 11 according to Eqs (18)-(21).

The evaluation grade can be obtained due to the maximum closeness degree T_i . To verify whether the excavation face has reached the critical condition for the instability, the evaluation results obtained by the stability coefficient method according to Eq.(1) are listed in Table 11 as well. The parameters C , δ_i , γ , C_U and δ_s in Eq. (1) are obtained from the geological exploration data. The parameter D can be found from the shield parameters.

Finally, the actual grade and the evaluation results of the excavation face stability obtained by the ideal point method and stability coefficient method are listed in Table 11. Table 11 shows that the evaluation results of the ideal point model are basically consistent with the actual situation. However, the results calculated by the classical coefficient method deviate from the actual grade. The results indicate that the ideal point model can be used to evaluate the stability of the excavation face of the cross-river shield tunnel.

5. Discussion

In this paper, the grading standard of the indexes for excavation face stability evaluation is obtained by discretizing the value range of the evaluation indexes. Although the support pressure and the grouting pressure are known to be important factors that affect excavation face stability, they are not selected as the indexes in this evaluation system according to the following reason. The support pressure is set according to the soil and water pressure in front of the excavation. However, the evaluation criteria of the influence degree of the supporting pressure on the excavation face stability are different in the areas with different geological conditions. The construction level is also a crucial evaluation index. Given the advanced construction technology and high comprehensive quality of the world's engineering construction technology, this factor is not selected as an evaluation index.

The weight calculation method is mainly divided into the subjective method and objective method. In this paper, the weights of evaluation indexes are rationally assigned by a comprehensive weight method. Moreover, the subjective and objective weights are acquired by AHP and entropy method respectively. The weight calculation results of the AHP are highly subjective, thus the entropy weight method is adopted to optimize the weight calculation results. Based on real data samples, the entropy weight method determines the weight of each index according to the amount of information contained in the decision-making system, which increases the objectivity of the weight calculation results. The calculation results indicate that the two weights have a large deviation, which shows that using the combined weight method to calculate the weight of the

indexes is very necessary.

On the basis of the related researches and experts' engineering experience, the description of the stability grade of the excavation face is given in Table 7. Based on the statistical data of the segment deformation obtained from the monitoring measurement, it can be concluded that the deformation of the segment is also a verification of the excavation face stability. Since the deformation of the segment is a process that accumulates over time, when the stability grade is 4 or 5, the deformation of the segment may not accurately reflect the actual situation of the excavation face. Therefore, the sensor parameters obtained from the cutter head should be attention to as well.

The influence of surface overload is considered in the evaluation process of the classical stability coefficient method, but the influence of water in the cross-river tunnel construction process is not considered. In this paper, it is assumed that the river above the tunnel is soil with an equivalent gravity in using the stability coefficient method. In the landside section, i.e samples 1 and 2 (Table 11), the evaluation results calculated by the classical stability coefficient method tend to be good, which is basically consistent with the ideal point evaluation model and the actual situation. In the river section, i.e samples 3-5 (Table 11), the result of the stability coefficient method is not consistent with the ideal point evaluation method or the actual situation.

6. Conclusions

Based on a comprehensive analysis of the geological conditions of the Yangtze River and the instability mechanism of the excavation face, seven evaluation indexes of the excavation face stability of shield tunneling are determined, namely, the over-span ratio e , tunnel depth h , soil permeability p , natural water content w , internal friction angle ϕ , cohesion of soil c , and the advancing speed v . The AHP-entropy weight method is used to determine the combination weight of the evaluation indexes. The results show that the weight of the over-span ratio e is the highest, while that of the tunnel depth h is the second-highest, and the weight of the cohesion of soil c is the lowest.

In this paper, a stability evaluation system for the excavation face is proposed by quantifying the evaluation index of the excavation face stability. For the description of the excavation face stability in Table 7, there may be differences in the description of the different tunnel environment, which again indicates that the stability of the excavation face is a relative concept. The stability of the excavation face is closely related to the actual geological conditions. Moreover, the deformation of the segment is an important characterization parameter for the stability of the excavation face. Since the collection of deformation data of the segment is a long-term process, the instability of the excavation surface occurs instantaneously. Therefore, more construction parameters, including the rotating speed of the cutter head and the support pressure, need to be noticed.

The stability grade of the excavation face during the actual construction process is given by establishing the excavation face stability evaluation system. Table 11 shows

that the evaluation results of the samples are basically consistent with the actual situation. The stability grade of sample 3 obtained by the stability coefficient method is V, which indicated the instability of the excavation face according to Table 1. However, the actual stability grade of sample 3 is III, which is in good agreement with the idea point method results. The result again shows the limitation of the stability coefficient method.

According to this case study, the prediction model is feasible for stability evaluation of the excavation face in the cross-river shield tunnel. However, the evaluation performance of the model needs to be improved. We can expand the number of the learning samples to conduct a more comprehensive database of the cross-river shield tunnel. Moreover, the descriptions of the stability grades can be standardized by engineering applications.

Acknowledgments

Much of the work presented in this paper was supported by the National Natural Science Foundation of China (grant numbers 51379112, 51422904, 41877239 and 41772298), and the State Key Development Program for Basic Research of China (grant number 2013CB036002), and Fundamental Research Funds for the Central Universities (grant number 2018JC044), and Natural Science Foundation of Shandong Province (grant number JQ201513). The authors would like to express appreciation to the reviewers for their valuable comments and suggestions that helped improve the quality of our paper.

References

- Aalianvari, A., Katibeh, H. and Sharifzadeh, M. (2012), "Application of fuzzy Delphi AHP method for the estimation and classification of Ghomrud tunnel from groundwater flow hazard", *Arab. J. Geosci.*, **5**(2), 275-284. <https://doi.org/10.1007/s12517-010-0172-8>.
- Ahmed, M. and Iskander, M. (2012), "Evaluation of tunnel face stability by transparent soil models", *Tunn. Undergr. Sp. Technol.*, **27**(1), 101-110. <https://doi.org/10.1016/j.tust.2011.08.001>.
- Anagnostou, G. and Kovári, K. (1996), "Face stability conditions with earth-pressure-balanced shields", *Tunn. Undergr. Sp. Technol.*, **11**(2), 165-173. [http://dx.doi.org/10.1016/0886-7798\(96\)00017-X](http://dx.doi.org/10.1016/0886-7798(96)00017-X).
- Attewell, P.B. and Boden, J.B. (1971), "Development of stability ratio for tunnels driven in clay", *Tunn. Tunn. Int.*, **3**(3), 195-198.
- Broms, B.B. and Benermark, H. (1967), "Stability of clay at vertical openings", *J. Soil Mech. Found. Eng. Div.*, **93**, 71-94.
- Chambon, P. and Corte, J.F. (1994), "Shallow tunnels in cohesionless soil: stability of tunnel face", *J. Geotech. Eng.*, **120**(7), 1148-1165. [http://dx.doi.org/10.1061/\(ASCE\)0733-9410\(1994\)120:7\(1148\)](http://dx.doi.org/10.1061/(ASCE)0733-9410(1994)120:7(1148)).
- Chen, R.P., Li, J., Kong, L.G. and Tang, L.J. (2013), "Experimental study on face instability of shield tunnel in sand", *Tunn. Undergr. Sp. Technol.*, **33**, 12-21. <https://doi.org/10.1016/j.tust.2012.08.001>.
- Coli, N., Pranzini, G., Alfi, A. and Boerio, V. (2008), "Evaluation of rock-mass permeability tensor and prediction of tunnel inflows by means of geostructural surveys and finite element seepage analysis", *Eng. Geol.*, **101**(3-4), 174-184. <https://doi.org/10.1016/j.enggeo.2008.05.002>.
- Constantin, M., Bednarik, M. Jurchescu, M.C. and Vlaicu, M. (2011), "Landslide susceptibility assessment using the bivariate statistical analysis and the index of entropy in the Sibiciu Basin (Romania)", *Environ. Earth Sci.*, **63**(2), 397-406. <https://doi.org/10.1007/s12665-010-0724-y>.
- Culí, L., Pujades, E., Vázquez-Suñé, E. and Jurado, A. (2016), "Modelling of the EPB TBM shield tunnelling advance as a tool for geological characterization", *Tunn. Undergr. Sp. Technol.*, **56**, 12-21. <http://dx.doi.org/10.1016/j.tust.2016.02.017>.
- Delgado, A. and Romero, I. (2016), "Environmental conflict analysis using an integrated grey clustering and entropy-weight method: A case study of a mining project in Peru", *Environ. Modell. Softw.*, **77**, 108-121. <https://doi.org/10.1016/j.envsoft.2015.12.011>.
- Dias, D. and Kastner, R. (2013), "Movements caused by the excavation of tunnels using face pressurized shields—analysis of monitoring and numerical modeling results", *Eng. Geol.*, **152**(1), 17-25. <https://doi.org/10.1016/j.enggeo.2012.10.002>.
- Duan, K., Wu, W. and Kwok, C.Y. (2018), "Discrete element modelling of stress-induced instability of directional drilling boreholes in anisotropic rock", *Tunn. Undergr. Sp. Technol.*, **81**, 55-67. <http://dx.doi.org/10.1016/j.tust.2018.07.001>.
- Felicísimo, Á.M., Cuartero, A., Remondo, J. and Quirós, E. (2013), "Mapping landslide susceptibility with logistic regression, multiple adaptive regression splines, classification and regression trees, and maximum entropy methods: a comparative study", *Landslides*, **10**(2), 175-189. <https://doi.org/10.1007/s10346-012-0320-1>.
- Hamidi, J.K., Shahriar, K., Rezai, B., Rostami, J. and Bejari, H. (2010), "Risk assessment based selection of rock TBM for adverse geological conditions using Fuzzy-AHP", *Bull. Eng. Geol. Environ.*, **69**(4), 523-532. <https://doi.org/10.1007/s10064-009-0260-8>.
- Hasanpour, R. (2014), "Advance numerical simulation of tunneling by using a double shield TBM", *Comput. Geotech.*, **57**, 37-52. <https://doi.org/10.1016/j.compgeo.2014.01.002>.
- Hatzor, Y.H., Wainshtein, I. and Mazor, D.B. (2010), "Stability of shallow karstic caverns in blocky rock masses", *Int. J. Rock Mech. Min. Sci.*, **47**(8), 1289-1303. <http://dx.doi.org/10.1016/j.ijrmms.2010.09.014>.
- Hong, E.S., Lee, I.M., Shin, H.S., Nam, S.W. and Kong, J.S. (2009), "Quantitative risk evaluation based on event tree analysis technique: Application to the design of shield TBM", *Tunn. Undergr. Sp. Technol.*, **24**(3), 269-277. <https://doi.org/10.1016/j.tust.2008.09.004>.
- Hyun, K.C., Min, S., Choi, H., Park, J. and Lee, I.M. (2015), "Risk analysis using fault-tree analysis (FTA) and analytic hierarchy process (AHP) applicable to shield TBM tunnels", *Tunn. Undergr. Sp. Technol.*, **49**, 121-129. <https://doi.org/10.1007/s12205-014-0538-7>.
- Jiang, Y.J. and Wu, X.Z. (2015), "Research progress and prospect of interaction between rock engineering and geo-environments", *J. Rock Mech. Geotech. Eng.*, **7**(6), 722-723. <https://doi.org/10.1016/j.jrmge.2015.06.012>.
- Katibeh, H. and Aalianvari, A. (2009), "Development of a New Method for Tunnel Site Rating from Groundwater Hazard Point of View", *J. Appl. Sci.*, **9**(8), 1496-1502. <https://doi.org/10.3923/jas.2009.1496.1502>.
- Khezri, N., Mohamad, H. and Fatahi, B. (2016), "Stability assessment of tunnel face in a layered soil using upper bound theorem of limit analysis", *Geomech. Eng.*, **11**(4), 471-492. <http://dx.doi.org/10.12989/gae.2016.11.4.471>.
- Kim D.I., Yoo, W.S., Cho, H. and Kang, K.I. (2014), "A fuzzy AHP-based decision support model for quantifying failure risk of excavation work", *KSCE. J. Civ. Eng.*, **18**(7), 1966-1976.

- <https://doi.org/10.1007/s12205-014-0538-7>.
- Kim, J., Salgado, R. and Lee, J. (2002), "Stability analysis of complex soil slopes using limit analysis", *J. Geotech. Geoenviron. Eng.*, **128**(7), 546-557. [https://doi.org/10.1061/\(ASCE\)1090-0241\(2002\)128:7\(546\)](https://doi.org/10.1061/(ASCE)1090-0241(2002)128:7(546)).
- Kim, K., Oh, J.Y., Lee, H. and Choi, H. (2018), "Critical face pressure and backfill pressure of shield TBM considering surface settlements of saturated clayey ground", *J. Kor. Tunn. Undergr. Sp. Assoc.*, **20**(2), 433-452. <https://doi.org/10.9711/KTAJ.2018.20.2.433>.
- Kong, F.M. and Shang, J.L. (2018), "A validation study for the estimation of uniaxial compressive strength based on index tests", *Rock Mech. Rock Eng.*, **51**(7), 2289-2297. <https://doi.org/10.1007/s00603-018-1462-9>.
- Lee, I.M., Lee, J.S. and Nam, S.W. (2004), "Effect of seepage force on tunnel face stability reinforced with multi-step pipe grouting", *Tunn. Undergr. Sp. Technol.*, **19**(6), 551-565. <http://dx.doi.org/10.1016/j.tust.2004.01.003>.
- Li, T.Z. and Yang, X.L. (2019), "Face stability analysis of rock tunnels under water table using Hoek-Brown failure criterion", *Geomech. Eng.*, **18**(3), 235-245. <https://doi.org/10.12989/gae.2019.18.3.235>.
- Li, X., Xue, Y.G., Qiu, D.H., Ma, X.M., Qu, C., Zhou, B.H. and Kong, F.M. (2019), "Application of data mining to lagging deformation prediction of the underwater shield tunnel", *Mar. Georesour. Geotechnol.* <https://doi.org/10.1080/1064119X.2019.1681039>.
- Li, Y., Emeriault, F., Kastner, R. and Zhang, Z.X. (2009), "Stability analysis of large slurry shield-driven tunnel in soft clay", *Tunn. Undergr. Sp. Technol.*, **24**(4), 472-481. <https://doi.org/10.1016/j.tust.2008.10.007>.
- Li, Z.Q., Xue, Y.G., Qiu, D.H., Xu, Z.H., Zhang, X.L., Zhou, B.H. and Wang, X.T. (2017), "AHP-ideal point model for large underground petroleum Storage Site Selection: An Engineering Application", *Sustainability.*, **9**(12), 2343. <https://doi.org/10.3390/su9122343>.
- Ma, X.D. and Zoback, M.D. (2018), "Static and dynamic response of Bakken cores to cyclic hydrostatic loading", *Rock Mech. Rock Eng.*, **51**(6), 1943-1953 <http://dx.doi.org/10.1007/s00603-018-1443-z>.
- Ma, X.L., Rudnicki, J.W. and Haimson, B.C. (2017), "Failure characteristics of two porous sandstones subjected to true triaxial stresses: applied through a novel loading path", *J. Geophys. Res. Sol. Earth*, **122**(4), 2525-2540. <https://doi.org/10.1002/2016JB013637>.
- Maynar, M.J. and Rodríguez, L.E. (2005), "Discrete numerical model for analysis of earth pressure balance tunnel excavation", *J. Geotech. Geoenviron. Eng.*, **131**(10), 1234-1242. [https://doi.org/10.1061/\(asce\)1090-0241\(2005\)131:10\(1234\)](https://doi.org/10.1061/(asce)1090-0241(2005)131:10(1234)).
- Perazzelli, P., Leone, T. and Anagnostou, G. (2014), "Tunnel face stability under seepage flow conditions", *Tunn. Undergr. Sp. Technol.*, **43**, 459-469, 1371-1374. <https://doi.org/10.1016/j.tust.2014.03.001>.
- Shin, Y.J., Kim, B.M., Shin, J.H. and Lee, I.M. (2010), "The ground reaction curve of underwater tunnels considering seepage forces", *Tunn. Undergr. Sp. Technol.*, **25**(4), 315-324. <https://doi.org/10.1016/j.tust.2010.01.005>.
- Shu, S.Z., Muhunthan, B. and Li, X.S. (2011), "Numerical Simulation of the Influence of Initial State of Sand on Element Tests and Micropile Performance", *Int. J. Geomech.*, **11**(5), 370-380. [https://doi.org/10.1061/\(ASCE\)GM.1943-5622.0000095](https://doi.org/10.1061/(ASCE)GM.1943-5622.0000095).
- Song, S.G., Tian, R.Z., Li, L.P., Hu, J., Shen, C.S. and Peng, S.Z. (2018), "Adaptability Study of EPB Shield Machine in Clay Stratum in Xuzhou", *Geotech. Geol. Eng.*, **37**(4), 2335-2341. <https://doi.org/10.1007/s10706-018-00759-z>.
- Sousa, R.L. and Einstein, H.H. (2012), "Risk analysis during tunnel construction using Bayesian Networks: Porto Metro case study", *Tunn. Undergr. Sp. Technol.*, **27**(1), 86-100. <https://doi.org/10.1016/j.tust.2011.07.003>.
- Srivastava, A., Babu, G.S. and Haldar, S. (2010), "Influence of spatial variability of permeability property on steady state seepage flow and slope stability analysis", *Eng. Geol.*, **110**(3-4), 93-101. <https://doi.org/10.1016/j.enggeo.2009.11.006>.
- Su, M.X., Wang, P., Xue, Y.G., Qiu, D.H., Li, Z.Q., Xia, T. and Li, G.K. (2019), "Prediction of risk in submarine tunnel construction by multi-factor analysis: A collapse prediction model", *Mar. Georesour. Geotechnol.*, 1-11. <https://doi.org/10.1080/1064119X.2018.1535635>.
- Viratjandr, C. and Michalowski, R.L. (2006), "Limit analysis of submerged slopes subjected to water drawdown", *Can. Geotech. J.*, **43**(8), 802-814. <https://doi.org/10.1139/t06-042>.
- Wang, Y.C., Zhao, N., Jing, H.W., Meng, B. and Yin, X. (2016), "A novel model of the ideal point method coupled with objective and subjective weighting method for evaluation of surrounding rock stability", *Math. Probl. Eng.*, <http://dx.doi.org/10.1155/2016/8935156>.
- Wu, W. and Zhao, J. (2015), "Effect of water content on P-wave attenuation across a rock fracture filled with granular materials", *Rock Mech. Rock Eng.*, **48**(2), 867-871. <http://dx.doi.org/10.1007/s00603-014-0606-9>.
- Zhang, B., Wang, X., Zhang, J.S. and Meng, F. (2017), "Three-dimensional limit analysis of seismic stability of tunnel faces with quasi-static method", *Geomech. Eng.*, **13**(2), 301-318. <https://doi.org/10.12989/gae.2017.13.2.301>.

CC